ACS OMEGA

http://pubs.acs.org/journal/acsodf

Article

Experimental Study of Preheated Secondary Air on the Performance of an Updraft Coal Heating Stove

Huaibin Gao,* Jianing Zhang, Shouchao Zong, Chuanwei Zhang, Hongjun Li, and Guanghong Huang

Cite This: *ACS Omega* 2022, 7, 46090−46098

Read Online

ACCESS | Metrics & More | Article Recommendations

ABSTRACT: Although the Chinese government encourages using clean fuels for heating, many households in remote areas still rely on coal as their energy, especially in the Qinghai Tibet Plateau. An updraft coal heating stove was modified to preheat secondary air. The performance of the modified stove was studied compared with a baseline stove. The temperatures in the combustion chamber and near the chimney exit are measured, and the undiluted exhaust concentrations of CO, NO_x, and SO_2 are obtained. The results indicated that the temperatures and exhaust gas concentrations varied periodically with the coal addition. The oxygen concentration in the flue gas for the modified stove is higher than that for the baseline stove, and the O_2 concentration was decreased with the increase in fuel feed rate. The CO concentration peaked 5−15 min after fuel addition and descended quickly toward a baseline with the higher fuel feed rates. It remained almost unchanged at the beginning and then slightly increased when the combustion began to fade with a lower fuel feed rate for the modified stove. The NO_x emission for the modified stove is generally lower than that for the baseline stove. The NO_x formation during coal combustion mainly comes from prompt NO and fuel NO, while the SO_2 emission is mainly related to the sulfur element in the raw coal in the present work. The modified stove is effective in reducing NO_x and SO_2 emissions. However, the CO emission of the modified stove is higher than that of the baseline stove, especially at the end of the batch.

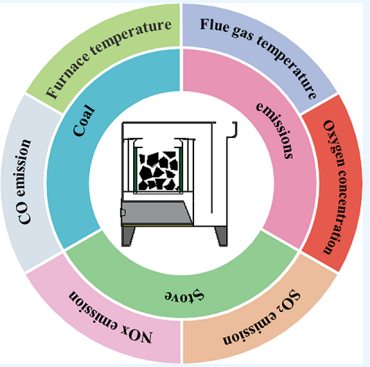

1. INTRODUCTION

Most households in rural areas of China are significantly dependent on coal or biomass for cooking and space heating, which accounts for a large proportion of air pollutant emissions such as CO, NO_x, SO_2, unburned hydrocarbons, and toxic organic compounds.[1−3] The magnitude and type of air pollution emissions resulting from combustion are sensitive to the combustion conditions, which are the precise physical and temporal relationships between the stove and the fuel. The environmental and public health concerns over coal emissions have motivated the coal research community to develop technologies that can reduce incidental emissions from incomplete coal combustion. A large number of improved coal stoves have been developed in different countries. Most of these aim to overcome the two major drawbacks of traditional stoves' low efficiency and indoor air pollution. Several designs have been proven effective in improving combustion efficiency, for example, rocket elbow stoves,[4] semi-gasifier stoves,[5−9] and thermoelectric stoves.[10−12]

The stove geometry (chimney height and chimney areas) also plays an important role in the performance of a stove by influencing the air-to-fuel ratio and, subsequently, the production of PM2.5 and CO emissions. The presence of a chimney generally resulted in lower PM2.5 and CO emissions.[13,14] Furthermore, Dorvlo et al.[15] evaluated the effect of two chimney configurations on the performance of a biomass cook stove. The results showed that the SS (the SS chimney has elbow joints) chimney configuration is suitable for a faster heating stove. In contrast, the ZS (the ZS chimney has a 90° angle at its joints) chimney maintains a higher overall internal stove temperature. Endriss et al.[16] showed that the draft influences temperature, while the particulate matter concentrations significantly decreased with the increase in draft. Mehta and Richards[17] experimentally studied a top-lit updraft cook stove and reported that the char remaining at the end of gasification decreased with the increased diameter of the combustion chamber. Guerrero et al.[18] showed that the particulate matter emission factors decreased by at least 20% using inert ceramic foams (silicon carbide) inside a wood stove combustion chamber.

Apart from the stove type and geometry, the fuel properties influence the emission and combustion efficiency. One relatively inexpensive method is to burn coal in formulated form instead of raw coal because the formulation of raw coal

Received: June 19, 2022
Accepted: November 30, 2022
Published: December 8, 2022

can enhance coal combustion efficiency and reduce air pollution emissions.[19,20] For instance, Shao et al.[21] reported that less particulate matter (PM) was emitted from burning honeycomb briquettes than from burning raw powdered coal. Kühn et al.[22] found a reduction of 80, 90, and 35% in PM, VOC, and SO_2 emissions, respectively, for low-smoke fuel compared to raw medium-rank bituminous coal. Makonese et al.[23] showed that an increase in coal moisture content led to a decrease in firepower, and the combustion efficiency increased by 25% with an increase in moisture content. Measured carbon monoxide (CO) emission factors increased with moisture content, while carbon dioxide (CO_2) emission factors remained unchanged. In addition, pollution reductions can be achieved by supplying a regulated graded coal size. Li et al.[24] found that the primary particulate matter (PM) emissions from household coal combustion decreased with increasing coal size. Masondo et al.[25] investigated the influence of the size of coal pieces on brazier emission performance and indicated that small and medium coal particle sizes produced comparable emissions (CO and PM2.5) and CO/CO_2 ratios. Liu et al.[26] indicated that the emission of PM2.5, SO_2, and CO_2 of semi-coke combustion in improved heating stoves was lower than the baseline of burning raw coal, and no significant changes were observed in NO_x and CO emissions. Zhao et al.[27] measured the effects of coal size on PM2.5 and 16 PAHs from a natural cross-draft stove. It indicated that decreasing the coal size enhanced thermal efficiency and reduced pollutant emissions. The effect of moisture content in fuel on the performance of a stove was also studied by previous works.[28,29] Results indicated that the CO and PM2.5 emissions were reduced with the increase in moisture content in fuel.

A more efficient stove design could reduce the exhaust emission exposure of a considerable portion of the population. Emission factors are also dependent on the operator's care and skill and on the resulting combustion. There is a need for more research not only to improve stove designs but also to understand how the operation of a stove will influence performance in terms of efficiency and emission of pollutants. An updraft stove with preheated secondary air was designed for a domestic heating stove. The temperature profiles and undiluted exhaust concentrations of CO, NO_x, and SO_2 were obtained and analyzed at different fuel feed rates.

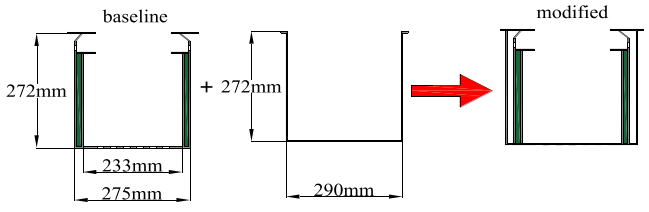

Figure 1. Stove chamber.

2. EXPERIMENTS

2.1. Experimental Setup. Figures 1 and 2 show the schematic diagram of the stove chamber and the space-heating stove, respectively. The schematic of the experimental setup is shown in Figure 3, which consists of a coal stove, thermocouples, a data acquisition system, and a flue gas analyzer. A household coal stove (80 cm long, 60 cm wide, and 60 cm high) for raw coal chunks was designed with a stainless-steel pipe of 10 cm diameter and 220 cm height as a chimney. The combustion chamber of the baseline stove consists of two concentric stainless-steel tubes with an interior diameter of 233 mm and an outer diameter of 275 mm (both 1.5 mm thick). The gap between the two cylinders is closed at the upper and lower end to provide an insulating air gap with no through flow. There is a cast iron grate at the bottom of the combustion chamber as a fuel holder and primary air inlet. Ninety-six holes with a diameter of 5 mm were drilled in four staggered rows around the top of the combustion chamber as the secondary air inlet. The raw coal chunks are ignited at the cast iron grate, and then the combustion zone moves upward through the porous fuel bed to heat and gasify the fuel. Primary air is provided through an opening in the stove's base, through the cast iron grate, and flows from the combustion zone to the pyrolysis zone. The secondary air is also provided from the base. It flows through the secondary air passage adjacent to the combustion chamber and enters the combustion chamber through the 96 secondary air inlets at the top of the combustion chamber. The width of the secondary air passage in the baseline stove is 150 mm (Figure 2a). The modified stove included another stainless tube diameter of 290 mm (thickness of 1.5 mm), forming a 6 mm secondary air passage adjacent to the outer wall of the combustion chamber (Figures 1 and 2). The outer diameter is constructed to form a closed space with the stove casing. By confining the airflow to a narrow space adjacent to the hot combustion chamber, the secondary air is heated to a higher temperature, leading to a lower density of flue gas and a larger natural draft. Additionally, the modification acts as an additional insulation layer for the combustion chamber. The flow rate and temperature of secondary air are the critical factor for CO. The gas temperature needs to remain above the CO auto-ignition temperature (605 °C) for as long as possible to ensure burn-out of residual carbon monoxide. Too much (unrestricted) secondary air will cool the gases and possibly reduce the concentration of CO below the lower flammability concentration (12% by volume), allowing the residual CO to be emitted. The flow rate and temperature of secondary air depend on the channel between the hot combustion chamber and the adjacent cylinder. A narrow channel will result in a lower flow rate and higher secondary air temperature. In contrast, a wide channel will lead to a higher flow rate and lower secondary air temperature.

Five K-type thermocouples were inserted to monitor the combustion chamber temperature, positioned every 50 mm starting from 20 mm above the cast iron grate. A data acquisition system (model MX 100) was used to measure and report the temperature of the combustion chamber. The gas probe was placed in the center of the vertical flue pipe with an attitude of 240 cm from the floor, and the real-time concentrations of NO_x, CO, and SO_2 in the flue gas were measured by a flue gas analyzer (Testo350, Sparta, Germany) and recorded at intervals of 5 min during the combustion period. The specifications of the flue gas analyzer are available in Table 1. However, the measured results are not useful for comparison purposes directly because the amount of excess air (EA) is uncontrolled. Hence, measured concentrations (ppm) have been recalculated and referenced to 0% excess oxygen. All concentrations in the corresponding figures refer to 0% excess O_2. The calculations are shown in eqs 1 and 2.

https://doi.org/10.1021/acsomega.2c03825
ACS Omega 2022, 7, 46090−46098

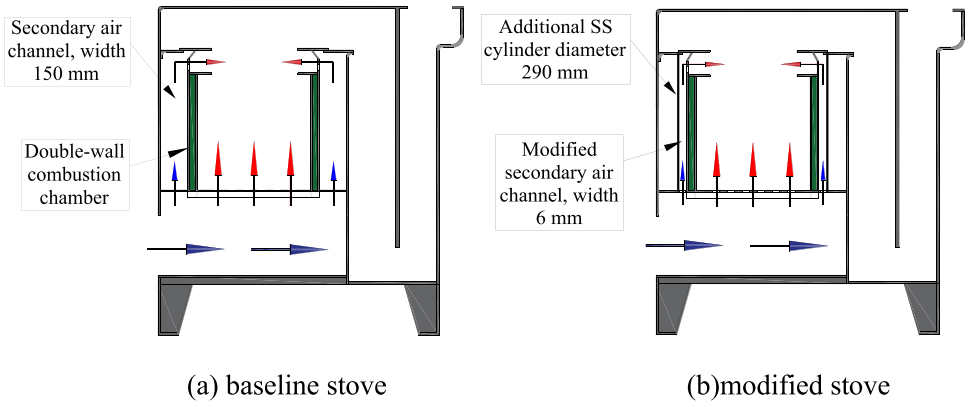

Figure 2. Schematic diagram of the space-heating stove. (a) Baseline stove and (b) modified stove.

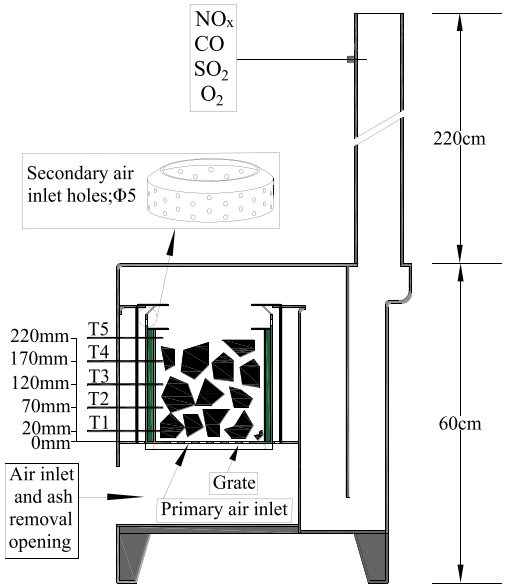

Figure 3. Experimental setup.

Table 1. Technical Data of the Flue Gas Analyzer

parameter	measurement range
O_2	0–25%
CO	0-10,000 ppm
NO	0-3000 ppm
NO_2	0-500 ppm
SO_2	0-5000 ppm
flue gas temperature	−40 to 1200 °C

$$\lambda = \frac{21}{21 - [\varphi'_{(O_2)} + \varphi'_{(CO)}]} \quad (1)$$

$$\rho = \rho' \cdot \lambda \quad (2)$$

where $\varphi'_{(O_2)}$, $\varphi'_{(CO)}$, λ, ρ', and $\rho$are the measured O_2, the measured CO, total air demand, gas concentration (ppm), and undiluted concentration (ppm), respectively.

2.2. Fuel Properties. The raw coal chunks with a diameter of 4−6 cm have been used as fuel throughout the experiments. The characterization of the fuel was measured before the test. ASTM D5373-2014 for elemental analysis (C and H); China standard methods GB/T 476-2008, GB/T 19227-2008, and GB/T 214-2007 for elemental analysis (O, N, and S); GB/T 213-2008 for LHV (lower calorific value) determination; GB/T 211-2007 for moisture; and GB/T 212-2008 for ash, chlorine, and sulfur concentration were used. The main characteristics of the coal fuel are summarized in Table 2. The carbon content in the coal fuel is 52.71%, and the lower heating value (LHV) is 22.28 MJ/kg.

Table 2. Properties of the Fuels Used

property	results	property	results
HHV (MJ/kg)	23.14	C (%)	61.79
LHV (MJ/kg)	22.28	H (%)	2.24
humidity (%)	14.30	O (%)	9.10
volatility (%)	21.54	N (%)	0.41
ash (%)	11.45	S (%)	0.71
carbon content (%)	52.71		

2.3. Experimental Procedure. A new batch of small coal chunks was used for each combustion sequence, starting with the stove at ambient temperature. After ignition, a pretest period was applied to develop a bed of glowing charcoal and for the stove to reach a stable operating temperature. The temperatures and pollutant emissions were measured and recorded before adding the first refueling. After preheating the combustion chamber, the prepared preweighed coal chunks were added to the stove for ignition by preburned coal without disturbance. Two further batches of coal were put into the stove when the combustion began to fade (fade, determined from trial burns to occur after 1 h). The inlet air opening was kept open and unchanged for all the different burn rates. The total recorded time for each test sequence was 3 h. The same test procedure was used for all test runs.

3. RESULTS AND DISCUSSION

Results are presented in two sections. First, comparisons are made between the baseline and modified stoves for each of the measured parameters: flue gas temperatures, flue gas oxygen, and the undiluted exhaust gas concentrations of CO, NO_x, and SO_2. These comparisons are made for a refueling rate of 2 kg/h, as shown in Figures 456789. Second, the effect of fuel feed rate on the performance of the modified stove is shown in Figures 101112131415.

3.1. Influence of Combustion Chamber Structure on Temperature Distributions and Emissions. *3.1.1. Temperature Distributions.* The modified stove with the modified double combustion chamber has been studied in the present

https://doi.org/10.1021/acsomega.2c03825
ACS Omega 2022, 7, 46090−46098

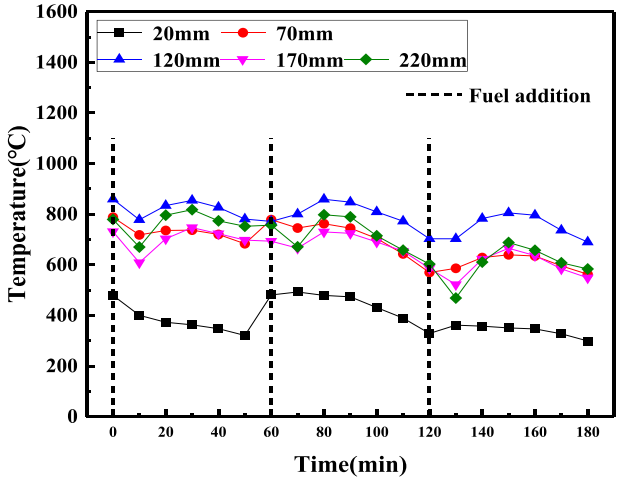

(a) baseline stove

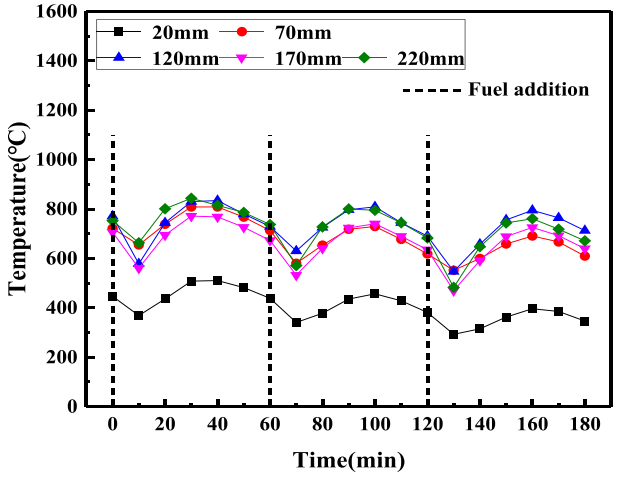

(b) modified stove

Figure 4. Temperature profiles for the (a) baseline and (b) modified stoves (2 kg/h).

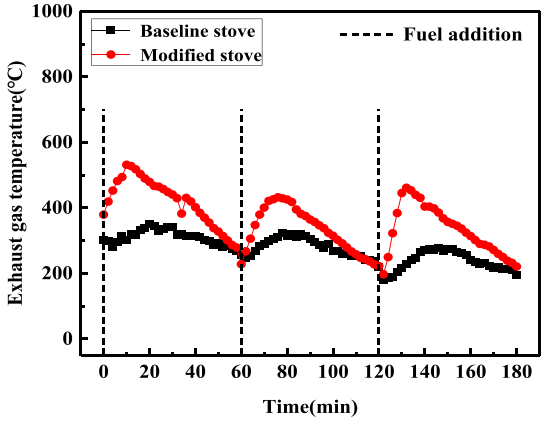

Figure 5. Temperature variation of flue gas for the baseline and modified stoves (2 kg/h).

work to obtain higher combustion efficiency and lower flue gas emissions for household heating. The comparative experiments were conducted for the baseline and modified stoves. The comparison of temperature profiles obtained from the baseline and modified stoves during the combustion sequences at a fuel

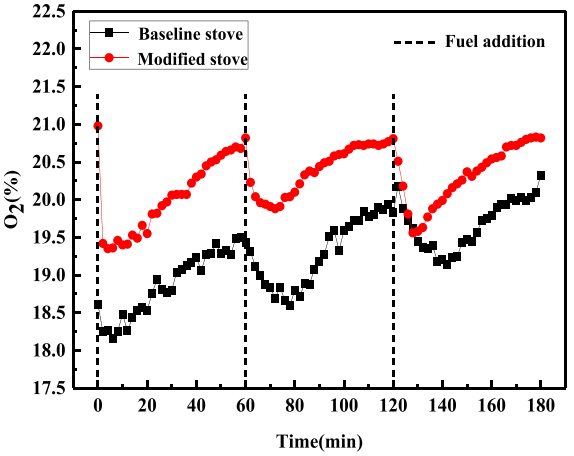

Figure 6. Oxygen concentration for the baseline and modified stoves (2 kg/h).

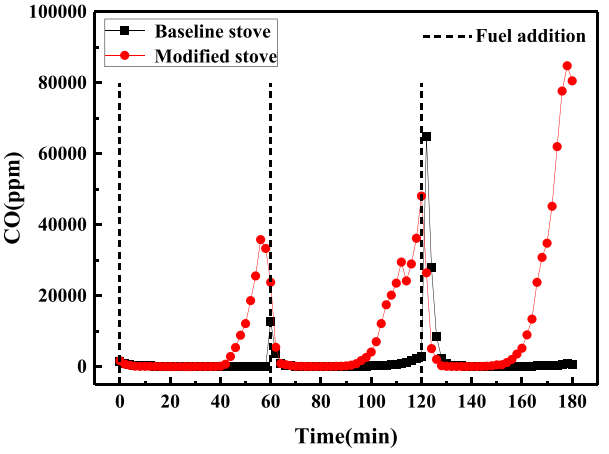

Figure 7. CO emission for the baseline and modified stoves (2 kg/h).

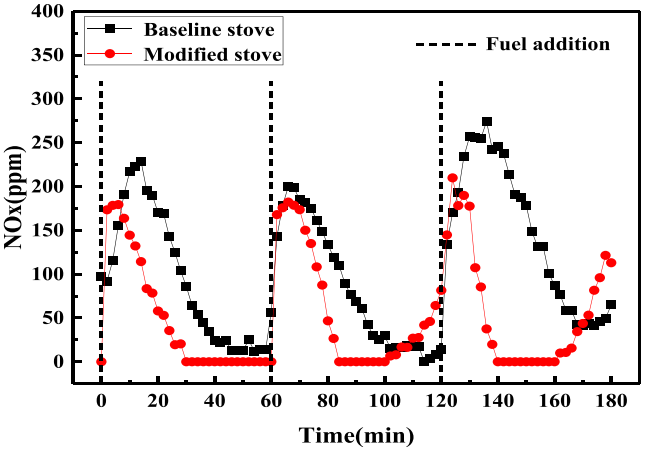

Figure 8. NO_x emission for the baseline and modified stoves (2 kg/h).

feed rate of 2 kg/h is shown in Figure 4. It can be seen that the temperatures varied periodically with the coal addition for both baseline and modified stoves. For every burn sequence of the baseline stove, temperatures decreased quickly after the addition of coal since more energy was needed to release the combustion gases. The minimum temperatures were reached after 5−15 min. Then, the temperatures increased slightly and

https://doi.org/10.1021/acsomega.2c03825
ACS Omega 2022, 7, 46090−46098

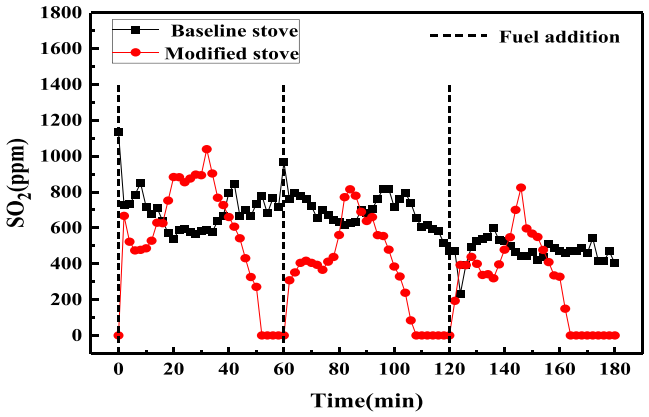

Figure 9. SO_2 emission for the baseline and modified stoves (2 kg/h).

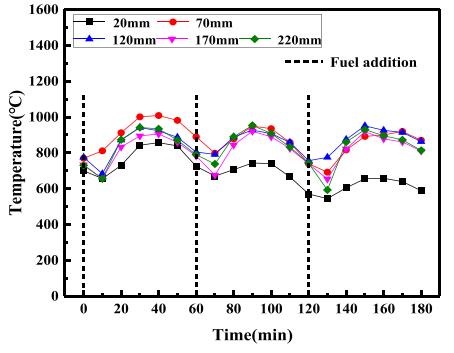

(a) 4.0 kg/h

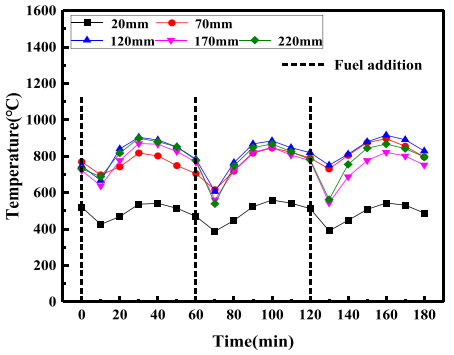

(b) 3.0 kg/h

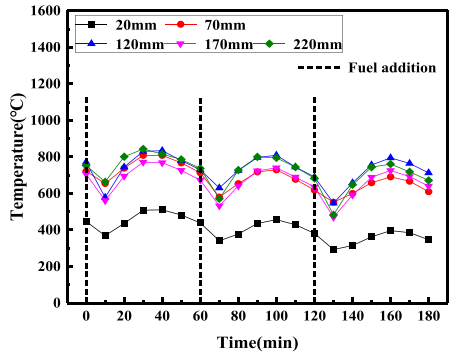

(c) 2.0 kg/h

Figure 10. Temperature profiles for different fuel additions in the modified stove: (a) 4.0 kg/h, (b) 3.0 kg/h, and (c) 2.0 kg/h.

reached peak values 35−45 min after coal addition. Similar tendencies can be seen in the modified stove. The temperature

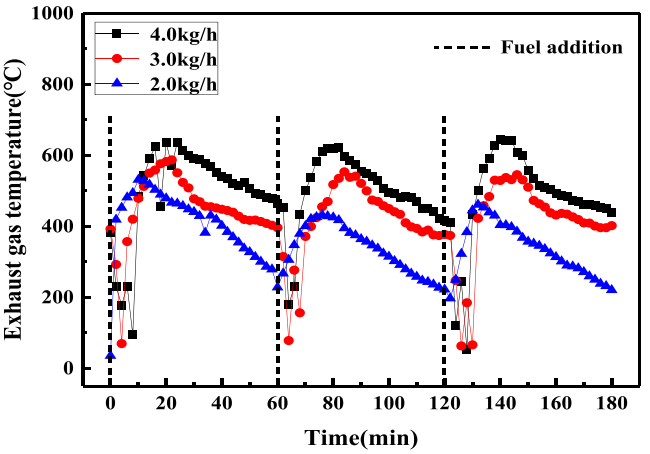

Figure 11. Temperature variation of flue gas for different fuel additions in the modified stove.

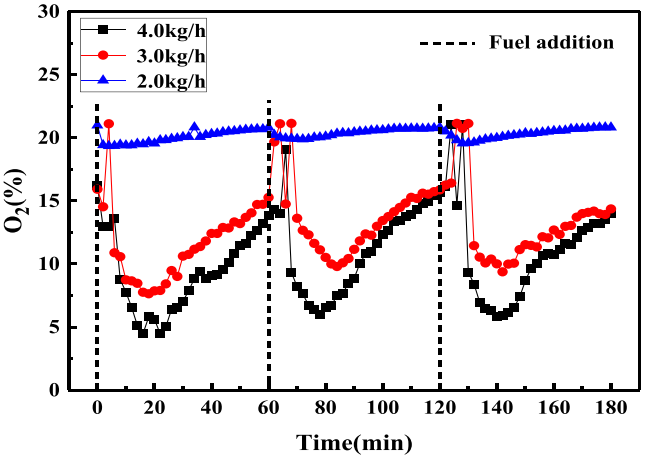

Figure 12. Oxygen concentration for different fuel additions in the modified stove.

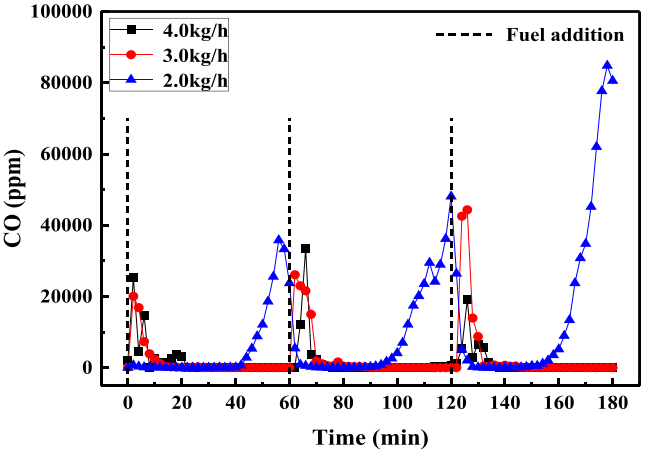

Figure 13. CO emission for different fuel additions in the modified stove.

descended quickly and reached the lowest values after 5−15 min and then increased slightly. Peak values were reached 25−35 min after the coal addition. The physical and chemical processes of fuel included drying, preheating, the pyrolytic release of volatile combustibles matter, and the combustion of the pyrolyzed and fixed carbon. The temperature fluctuation

https://doi.org/10.1021/acsomega.2c03825
ACS Omega 2022, 7, 46090−46098

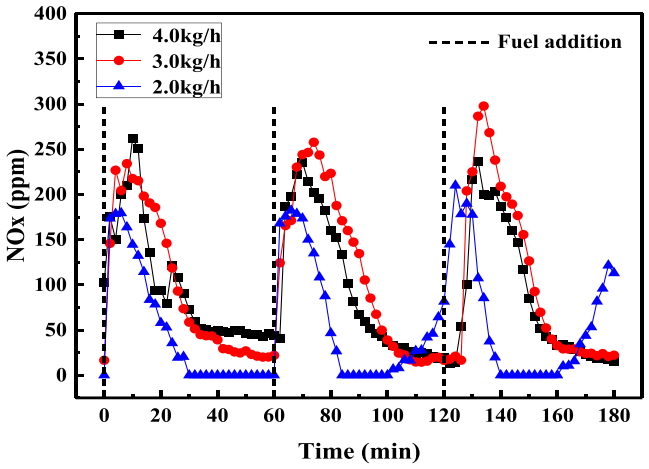

Figure 14. NO_x emission for different fuel additions in the modified stove.

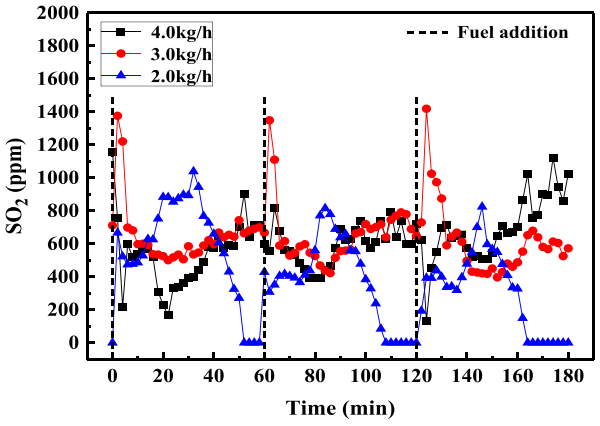

Figure 15. SO_2 emission for different fuel additions in the modified stove.

range of the baseline stove is smaller than that of the modified stove. The modified stove's insulation is better than the baseline stove's, which leads to a higher temperature, faster burn rate, and rapid heat release. The secondary air in the modified stove was better heated, and more energy was released in the combustion chamber. The lowest temperature was at the bottom of the combustion chamber. This is because the fuel put on the top of the combustion char leads first to burn out of coal and then ash agglomeration above the baffle.

Figure 5 displays the temperature variation of flue gas during the whole burn sequence at a fuel feed rate of 2 kg/h. The flue gas temperature rapidly increased to 354 and 531 °C at the beginning and then slowly declined after the fuel addition for both the baseline stove and modified stove, respectively. This is explained by the rapid pyrolytic release and combustion of volatile combustible matter after the addition of coal due to the higher temperature of the fuel bed. The decreasing flue gas temperature at the end of the burn sequence showed that the entire coal bed had gasified, and the fixed carbon began to burn. Furthermore, the modified stove reached the peak gas temperature faster than the baseline stove. This is because the volatile gases are released, and more heat is output due to the preheated secondary air and the better insulation of the modified stove. The flue gas temperature for the modified stove was higher than that of the baseline stove. More heat will exit from the chimney with a higher flue gas temperature, resulting in lower heat transfer to the room space.

3.1.2. Oxygen Contents. Excess oxygen/air in flue gas is an essential index for efficiency, which will carry heat released from coal combustion and remove it from the stove. Figure 6 displays the variation of oxygen concentration during the whole burn sequence for the two baseline and modified stoves at a fuel feed rate of 2 kg/h. The O_2 concentrations changed periodically with the coal addition for the two stoves due to the temperature variation. The O_2 concentration suddenly decreases after the fuel addition due to the lower natural draft and higher flow resistance across the combustion chamber and then slowly increases with the increasing temperature and decreasing flow resistance as the combustion proceeds. The O_2 concentration in the flue gas varied from 19.3 to 20.7% and 18.3 to 19.7% for the two stoves. The O_2 concentration for the baseline stove is lower than that of the modified stove. This is because the natural draft of stove is significantly influenced by the chimney draft, which depends on the flue gas temperature, the chimney characteristics, and the weather conditions. The airflow rate is controlled by the pressure that draws air into the combustion chamber and discharges from the chimney. It is mainly related to chimney height and the density difference between the flue gas and ambient air, as shown in eq 3 (ASHRAE, 2012)[30]

$$m_{total} = A_{cs}\left(\frac{2 \times g \times Z}{k}\right)^{0.5} (\rho_{flue}(\rho_{amb} - \rho_{flue}))^{0.5} \quad (3)$$

where m_{total}, A_{cs}, Z, k, g, ρ_{flue}, and ρ_{amb} are the total mass flow rate of air, the cross-sectional area of the chimney, chimney height, gravitational acceleration, and density of flue gas and ambient air, respectively. The natural draft and airflow rate are increased with the increased temperature of flue gas as the gas density is highly dependent on temperature. The corresponding flue gas losses have a similar tendency, while the combustion efficiency has the opposite trend.

3.1.3. CO Emissions. Carbon monoxide (CO) is a hazardous primary product of incomplete combustion, which mainly depends on mixing, residence time, and combustion temperature. Figure 7 displays the variations of CO emission during the whole burn sequence for the two stoves at a fuel feed rate of 2 kg/h. The burn sequence in a coal-fired stove is generally divided into the startup stage, steady-state stage, and burnout stage. At startup, the combustible gas increased immediately after, with the CO emission similar for the two stoves. During the burnout phases, fuel volatiles were exhausted and partial combustion occurred. CO emissions increased for the modified stove when the combustion began to fade at the end of the batch. This is because the total airflow rate and the proportion of secondary air decreased. The fuel layer became thinner, and the porosity of the packed bed increased, leading to a lower resistance for the primary air. However, secondary airflow resistance did not change significantly during the combustion process.

Furthermore, the burn rate of the modified stove was faster than that of the baseline stove due to the higher secondary air temperature and the better insulation of the combustion chamber. It requires a shorter time for the modified stove to burn out. Thus, the CO emissions increased again with the decreasing secondary airflow rate during the burnout period. The results also indicated that fuel was burned faster in the modified stove than in the baseline stove. Thus, the refueling

https://doi.org/10.1021/acsomega.2c03825
ACS Omega 2022, 7, 46090−46098

frequency should be increased, or the fuel mass per hour should be increased for the modified stove. It is proposed that the optimal design of a clean-combustion coal stove should focus on the air supply and mixing conditions at the initial stage of coal combustion. The fuel had to be added to continue the batch after the char was burnt.

3.1.4. NO_x Emissions. Figure 8 displays the variations of NO_x emission during the whole burn sequence for the two stoves at a fuel feed rate of 2 kg/h. The mechanism of NO_x formation generally originates from thermal NO, prompt NO, and fuel NO. The thermal NO is produced when the combustion temperature exceeds 1300 °C, while the prompt NO is formed with more hydrocarbon CH and relatively low oxygen concentration. The NO_x concentrations are first increased and then decreased after fuel addition. The maximum temperature for both baseline and modified stoves are below 1000 °C. Thus, the NO_x formation during coal combustion mainly comes from prompt NO and fuel NO in the present work. The hydrocarbon CH rapidly increases and the O_2 concentration suddenly decreases after the fuel addition. The NO_x emission for the baseline stove is generally higher than that for the modified stove during the combustion sequence. This is because the O_2 concentration for the modified stove is higher than for the baseline stove, as shown in Figure 6. More air was entering the combustion chamber due to the higher temperature of the modified stove, resulting in a lower NO_x concentration.

3.1.5. SO_2 Emissions. The SO_2 emission is mainly related to the sulfur element in the raw coal. It is noted that the SO_2 emission in flue gas is significantly dependent on the combustion temperature, the content of sulfur in raw coal, and the concentration of oxygen. The sulfur is emitted as either H_2S or SO_2. Figure 9 displays the variations of SO_2 emission during the whole burn sequence for the two stoves at a fuel feed rate of 2 kg/h. Compared to NO_x emission, the overall SO_2 concentrations in the flue gas are higher due to the higher sulfur content in the coal (0.71% by mass in Table 2). The SO_2 concentrations initially increase and then decrease after fuel addition for the modified stove. The SO_2 emission for the baseline stove is generally higher than that of the modified stove after adjusting to zero excess air (that is 0% oxygen).

3.2. Influence of Fuel Addition on Temperature Distributions and Emissions. *3.2.1. Temperature Distributions.* Similar experiments were conducted for the modified stove to study the influence of fuel feed rate on combustion performance. A comparison of temperature profiles obtained for different fuel feed rates in the modified stove is shown in Figure 10. The temperatures varied periodically with the coal addition. The temperature descended quickly and reached a minimum 5−15 min after coal addition and then increased slightly, reaching a maximum after 35−45 min. It is noted that the tendency of temperature fluctuation for different fuel feed rates is almost the same. In contrast, the highest and average temperatures in the combustion chamber increased with an increasing fuel feed rate. This is because the heat loss is almost the same due to the same insulation structure, while the energy entering the combustion chamber are different for various fuel feed rates.

Figure 11 displays the temperature variation of flue gas during the burn sequence for different fuel feed rates. The flue gas temperature rapidly increased and then slowly declined after the fuel addition. After adding coal, volatile combustible matter is released rapidly during pyrolysis due to the higher temperature of the fuel bed. The volatiles combust efficiently with the preheated secondary air, leading to increased flue gas temperatures. The decreasing flue gas temperature at the end of the burn sequence showed that the entire fuel load had gasified, and the fixed carbon began to burn. The temperature of flue gas increased with the increase in fuel feed rate. This is due to the larger feed rate that releases more volatile gases, in turn generating more heat.

3.2.2. Oxygen Contents. Figure 12 displays the variation of oxygen concentration during the burn sequence with different fuel feed rates for the modified stove. The O_2 concentrations were changed periodically for different fuel feed rates due to the temperature variation. The fluctuation range of O_2 concentration is increased with the increase in fuel feed rate. This is because a coal stove operated with a natural draft is strongly influenced by the flue gas temperature, the resistance of the combustion bed, and the chimney characteristics. The O_2 concentration suddenly decreased after the fuel addition due to the lower natural draft caused by the lower temperature in the combustion chamber. The O_2 concentration then slowly increased with the increasing temperature and decreasing flow resistance as the combustion proceeded. Moreover, the O_2 concentration was decreased with the increase in fuel feed rate. This is because the O_2 concentration depended on the natural draft and the flow resistance across the fuel bed. The natural draft was decreased while the flow resistance was increased with the increase in fuel feed rate due to the thicker packed bed of coal in the combustion chamber.

3.2.3. CO Emissions. The variations of the CO concentration at different fuel feed rates during the burn sequences for the modified stove are shown in Figure 13. The CO concentration peaked 5−15 min after fuel addition and descended quickly toward a baseline for the higher fuel feed rates (3 and 4 kg/h). This is because more combustible gas and volatile flammable matter were generated and discharged into the combustion zone when more coal was added and heated by the hot charcoal. On the other hand, the airflow rate suddenly decreased due to the higher flow resistance of the fuel bed for higher fuel feed rates. The CO emissions decreased when the combustion began to fade for the higher fuel feed rate due to the higher temperature and excess oxygen in the combustion chamber. However, the CO concentration remained almost unchanged at the beginning and then slightly increased when the combustion began to fade for the lower fuel feed rate (2 kg/h). This is because of the lower combustible gas and relatively higher airflow rate caused by the lower flow resistance of the fuel bed at the startup. Meanwhile, the total airflow rate and the proportion of secondary air declined at the end of the burn sequence due to the thinner layer of the fuel bed.

3.2.4. NO_x Emissions. Figure 14 displays the variation of NO_x concentration during the burn sequence with different fuel feed rates for the modified stove. Similarly, the NO_x concentrations increased initially and then decreased after fuel addition. The NO_x formation during coal combustion mainly comes from prompt NO and fuel NO. The fluctuation of NO_x concentration was smaller for lower fuel feed rates than for higher fuel feed rates. This is because a lower fuel feed rate means less nitrogen entering the combustion chamber during the burn sequence. Moreover, more prompt NO was formed due to the relatively higher hydrocarbon CH and lower oxygen concentration after the fuel addition. However, the NO_x

https://doi.org/10.1021/acsomega.2c03825
ACS Omega 2022, 7, 46090−46098

emissions of 4.0 kg/h addition are almost the same as those of 3.0 kg/h addition due to the almost identical natural draft.

3.2.5. SO_2 Emissions. Figure 15 shows the variations of the SO_2 concentration for different fuel feed rates for the modified stove. Total emissions of SO_2 were higher than for NO_x because of the higher sulfur content in the fuel (0.71% by mass, Table 2). The SO_2 concentrations initially increased and then decreased after fuel addition for the modified stove. The fluctuation range of SO_2 concentration for the lowest fuel feed rate (2 kg/h) is larger than for the higher fuel feed rates (3 and 4 kg/h).

4. CONCLUSIONS

A modified stove was designed to incorporate enhanced secondary air heating. The performance was studied compared with the baseline stove. The results showed that emissions varied periodically with fuel additions, and the temperatures increased with the increasing fuel feed rate. The insulation of the combustion chamber in the modified stove is better than that of the baseline stove, which leads to a higher temperature, faster burn rate, and rapid heat release. The NO_x and SO_2 emissions of the modified stove are dwindled compared with those of the baseline stove when the width of the secondary air channel is decreased. The O_2 concentration in the flue gas for the modified stove is higher than that for the baseline stove, and the O_2 concentrations decreased with increasing fuel feed rates. The CO concentration peaked 5−15 min after fuel additions and descended quickly toward a baseline for the higher fuel feed rates (3 and 4 kg/h). It remained almost unchanged at the beginning and then slightly increased when the combustion began to fade for the modified stove's lowest fuel feed rate (2 kg/h). NO_x formation during coal combustion mainly comes from prompt NO and fuel NO. The NO_x emissions for the modified stove are generally lower than those of the baseline stove during the combustion sequence. The SO_2 emissions are mainly related to the sulfur element in the raw coal. Unfortunately, the combustion chamber with a double concentric stainless-steel tube is easily corroded by sulfur in the coal, and a non-corrosive coating chamber should be developed in the future. Comparative field measurements of emission and combustion characteristics will be conducted at the Qinghai Tibet Plateau regions in upcoming experiments to validate the combustion chamber of the present updraft space-heating stove.

AUTHOR INFORMATION

Corresponding Author

Huaibin Gao − *School of Mechanical Engineering, Xi'an University of Science and Technology, Xi'an, Shaanxi 710054, China;* orcid.org/0000-0002-1931-0418; Email: gaohuaibin@xust.edu.cn

Authors

Jianing Zhang − *School of Mechanical Engineering, Xi'an University of Science and Technology, Xi'an, Shaanxi 710054, China*

Shouchao Zong − *School of Mechanical Engineering, Xi'an University of Science and Technology, Xi'an, Shaanxi 710054, China*

Chuanwei Zhang − *School of Mechanical Engineering, Xi'an University of Science and Technology, Xi'an, Shaanxi 710054, China*

Hongjun Li − *Special Equipment Research Institute of Xi'an, Xi'an, Shaanxi 710032, China*

Guanghong Huang − *Special Equipment Research Institute of Xi'an, Xi'an, Shaanxi 710032, China*

Complete contact information is available at: https://pubs.acs.org/10.1021/acsomega.2c03825

Notes

The authors declare no competing financial interest.

ACKNOWLEDGMENTS

This work was supported by the National Natural Science Foundation of China (52176132), the Natural Science Foundation of Shaanxi Province of China (2018JM5077, 2019JQ-795), and the Innovation Capability Support Program of Shaanxi (2021TD-27).

REFERENCES

(1) Bond, T. C.; Covert, D. S.; Kramlich, J. C.; Larson, T. V.; Charlson, R. J. Primary particle emissions from residential coal burning: Optical properties and size distributions. *J. Geophys. Res.: Atmos.* **2002**, *107*, 8347.

(2) Wang, S. X.; Zhao, B.; Cai, S. Y.; Klimont, Z.; Nielsen, C. P.; Morikawa, T.; Woo, J. H.; Kim, Y.; Fu, X.; Xu, J. Y.; et al. Emission trends and mitigation options for air pollutants in East Asia. *Atmos. Chem. Phys.* **2013**, *14*, 2601−2674.

(3) Chen, Y. J.; Sheng, G. Y.; Bi, X. H.; Feng, Y. L.; Mai, B. X.; Fu, J. M. Emission factors for carbonaceous particles and polycyclic aromatic hydrocarbons from residential coal combustion in China. *Environ. Sci. Technol.* **2005**, *39*, 1861−1867.

(4) Jetter, J. J.; Kariher, P. Solid-fuel household cook stoves: characterization of performance and emissions. *Biomass Bioenergy* **2009**, *33*, 294−305.

(5) Lai, A.; Shan, M.; Deng, M.; Carter, E.; Yang, X. D.; Baumgartner, J.; Schauer, J. Differences in chemical composition of PM2.5 emissions from traditional versus advanced combustion (semi-gasifier) solid fuel stoves. *Chemosphere* **2019**, *233*, 852−861.

(6) Baumgartner, J.; Clark, S.; Carter, E.; Lai, A. M.; Zhang, Y. X.; Shan, M.; Schauer, J. J.; Yang, X. D. Effectiveness of a household energy package in improving indoor air quality and reducing personal exposures in rural China. *Environ. Sci. Technol.* **2019**, *53*, 9306−9316.

(7) Jetter, J.; Zhao, Y.; Smith, K. R.; Khan, B.; Yelverton, T.; Dcarlo, P.; Hays, M. D. Pollutant emissions and energy efficiency under controlled conditions for household biomass cookstoves and implications for metrics useful in setting international test standards. *Environ. Sci. Technol.* **2012**, *46*, 10827−10834.

(8) Carter, E. M.; Shan, M.; Yang, X.; Li, L.; Baumgartner, J. Pollutant emissions and energy efficiency of Chinese gasifier cooking stoves and implications for future intervention studies. *Environ. Sci. Technol.* **2014**, *48*, 6461−6467.

(9) Tryner, J.; Willson, B. D.; Marchese, A. J. The effects of fuel type and stove design on emissions and efficiency of natural-draft semi-gasifier biomass cookstoves. *Energy Sustainable Dev.* **2014**, *23*, 99−109.

(10) Gao, H. B.; Huang, G. H.; Li, H. J.; Qu, Z. G.; Zhang, Y. J. Development of stove-powered thermoelectric generators: a review. *Appl. Therm. Eng.* **2016**, *96*, 297−310.

(11) Sornek, K.; Filipowicz, M.; Żołądek, M.; Kot, R.; Mikrut, M. Comparative analysis of selected thermoelectric generators operating with wood-fired stove. *Energy* **2019**, *166*, 1303−1313.

(12) Zheng, Y.; Hu, J.; Li, G.; Zhu, L. Y.; Guo, W. W. Testing and optimizing a stove-powered thermoelectric generator with fan cooling. *Materials* **2018**, *11*, 966.

(13) Roden, C. A.; Bond, T. C.; Conway, S.; Pinel, A. B. O.; MacCarty, N.; Still, D. Laboratory and field investigations of particulate and carbon monoxide emissions from traditional and improved cookstoves. *Atmos. Environ.* **2009**, *43*, 1170−1181.

(14) Prapas, J.; Baumgardne, R. M. E.; Marchese, A. J.; Willson, B.; Defoort, M. Influence of chimneys on combustion characteristics of buoyantly driven biomass stoves. *Energy Sustainable Dev.* **2014**, *23*, 286−293.
(15) Dorvlo, S. Y.; Addo, A.; Kemausuor, F.; Abenney-Mickson, S.; Ahrenfeldt, S.; Henriksen, U. Evaluating the effect of two chimney configurations on the overall airflow and heat transfer of a biomass cook stove. *J. Clean Energy Technol.* **2018**, *6*, 353−356.
(16) Endriss, F.; Grammer, P.; Russ, M.; Thorwarth, H. Impact of chimney-draught conditions on combustion and emission behavior of a wood-burning stove. *Chem. Ing. Tech.* **2021**, *93*, 412−420.
(17) Mehta, Y.; Richards, C. Gasification performance of a top-Lit updraft cook stove. *Energies* **2017**, *10*, 1529.
(18) Guerrero, F.; Arriagada, A.; Muñoz, F.; Silva, P.; Ripoll, N.; Toledo, M. Particulate matter emissions reduction from residential wood stove using inert porous material inside its combustion chamber. *Fuel* **2021**, *289*, No. 119756.
(19) Ge, S.; Xu, X.; Chow, J. C.; Watson, J.; Sheng, Q.; Liu, W. L.; Bai, Z. P.; Zhu, T.; Zhang, F. J. Emissions of air pollutants from household stoves: honeycomb coal versus coal cake. *Environ. Sci. Technol.* **2004**, *38*, 4612−4618.
(20) Zhi, G. R.; Chen, Y. J.; Feng, Y. L.; Xiong, S. C.; Li, J.; Zhang, G.; Sheng, G. Y.; Fu, J. M. Emission characteristics of carbonaceous particles from various residential coal-stoves in China. *Environ. Sci. Technol.* **2008**, *42*, 3310−3315.
(21) Shao, L. Y.; Hou, C.; Geng, C. M.; Liu, J. X.; Hu, Y.; Wang, J.; Tim, J.; Zhao, C. M.; Berube, K. The oxidative potential of PM10 from coal, briquettes and wood charcoal burnt in an experimental domestic stove. *Atmos. Environ.* **2016**, *127*, 372−381.
(22) Kühn, T.; Bunt, J. R.; Neomagus, H. W. J. P.; Piketh, J. S.; Everson, R. C.; Coetzee, S. Coal-derived low smoke fuel assessment through coal stove combustion testing. *J. Anal. Appl. Pyrolysis* **2017**, *126*, 158−168.
(23) Makonese, T.; Masekameni, D. M.; Annegarn, H. J. Influence of coal properties on the performance of fixed-bed coal-burning braziers. *J. Energy South. Afr.* **2017**, *28*, 40−51.
(24) Li, Q.; Jiang, J. K.; Zhang, Q.; Zhou, W.; Cai, S. Y.; Duan, L.; Ge, S.; Hao, J. M. Influences of coal size, volatile matter content, and additive on primary particulate matter emissions from household stove combustion. *Fuel* **2016**, *182*, 780−787.
(25) Masondo, L.; Masekameni, D.; Makonese, T.; Annegarn, H. J.; Kenneth, M. Influence of coal-particle size on emissions using the top-lit updraft ignition method. *Clean Air J.* **2016**, *26*, 15−20.
(26) Liu, Y.; Zhang, Y.; Li, C.; Bai, Y.; Zhang, D.; Xue, C.; Liu, G. Air pollutant emissions and mitigation potential through the adoption of semi-coke coals and improved heating stoves: Field evaluation of a pilot intervention program in rural China. *Environ. Pollut.* **2018**, *240*, 661−669.
(27) Zhao, N.; Li, B.; Chen, D.; Bahargul, Y.; Wang, R.; Zhou, Y.; Annegarn, H. J.; Pemberton-Pigott, C.; Dong, R.; Ju, X. The effect of coal size on PM2. 5 and PM-bound polycyclic aromatic hydrocarbon (PAH) emissions from a domestic natural cross-draft stove. *J. Energy Inst.* **2020**, *93*, 542−551.
(28) Yuntenwi, E. A. T.; MacCarty, N.; Still, D.; Ertel, J. Laboratory study of the effects of moisture content on heat transfer and combustion efficiency of three biomass cook stoves. *Energy Sustainable Dev.* **2008**, *12*, 66−77.
(29) Huangfu, Y. B.; Li, H. X.; Chen, X. F.; Xue, C. Y.; Chen, C.; Liu, G. Q. Effects of moisture content in fuel on thermal performance and emission of biomass semi-gasified cookstove. *Energy Sustainable Dev.* **2014**, *21*, 60−65.
(30) ASHRAE. *2012 Ashrae Handbook: heating, ventilating, and air-conditioning systems and equipment. inch-pound edition*. ASHRAE; 2012.

https://doi.org/10.1021/acsomega.2c03825
ACS Omega 2022, 7, 46090−46098